 CMC, vol.44, no.2, pp.105-122, 2014

Thermo-elastic Stresses in a Functional Graded Material under Thermal Loading, Pure Bending and Thermo-mechanical Coupling

Wei Zhang[1,2], Pengcheng Ni[2] and Bingfei Liu[1,3]

Abstract: Analytical expressions have been derived for the through thickness stresses of a Functional graded materials (FGMs) thin plate subjected to thermal loading, pure bending and thermo-mechanical coupling, respectively. The structure is comprised of a metallic layer, a ceramic layer and a functional graded layer. Continuous gradation of the volume fraction in the FGM layer is modeled in the form of an "m" power polynomial of the coordinate axis in thickness direction of the plate. Numerical scheme of discretizing the continuous FGM layer with different graded distributions such as linear (m=1), quadratic (m=2) and square root (m=0.5) has been developed by the averaging technique of composites. Solutions for the stress distributions have been derived for the system under thermal loading, pure bending and thermo-mechanical coupling, respectively.

Keywords: Theoretical solution, Functional graded materials, Thermo-mechanical coupling.

1 Introduction

Functionally graded materials (FGMs), as one kind of the functionally materials, are formed of two or more constituent phases with a continuously variable composition. FGMs shows many excellent merits in engineering applications such as the reduction of the in-plane stresses and stress intensity factors of a composite, and improved thermal properties, residual stress and the fracture toughness [Aboudi, Pindera, and Arnold (1994); Chakraborty, Gopalakrishnan and Reddy (2003); Sarkar, Datta and Nicholson (1997); Zimmerman and Lutz (1999)]. Due to this interest, a number of researches on both theoretical and experimental work dealing with

[1] Airport College, Civil Aviation University of China, Tianjin, 300300, China.
[2] Sino-European Institute of Aviation Engineering, Civil Aviation University of China, Tianjin, 300300, China.
[3] Corresponding author. Tel.: +1-86-2224092477; E-mail: bfliu@cauc.edu.cn

various aspects of FGM have been published in recent years including mechanics, manufacturing, applications and the thermal properties [Bishay and Atluri (2013); Birman and Byrd (2007); Dong, El-Gizawy, Juhany and Atluri (2014); Dong, El-Gizawy, Juhany and Atluri (2014); El-Hadek and Tippur (2003); Huang, Yao and Wang (2011); Liu, Dui and Yang (2013); Sun, Hong and Yuan (2014); Wu, He and Li (2002); Yang, Gao and Chen (2010)].

The designation and fabrication of the FGMs to achieve unique microstructures have already been launched [Miyamoto, Kaysser, Rabin, Kawasaki and Ford (1999)], and many analytical investigations have been conducted on the behaviors of FGM materials under thermal or mechanical loadings. As for the research on FGM beams, Librescu et al. [Librescu, Oh and Song (2005)] studied the behavior of thin walled beams made of FGM operating at high temperatures, in which the vibration and instability analysis along with the effects of volume fraction and temperature gradients were considered. The averaging technique of composite was utilized in [Liu, Dui and Yang (2013)], the effective stresses of each phase in a FGM beam under thermal loadings were calculated to judge the plasticity of the whole system, and the stress distributions of the whole material were obtained. [Yang, Chen, Xiang and Jia (2008)] studied both the free and forced vibrations of an FGM beam with variable thickness under thermally induced initial stresses based on the Timoshenko beam theory. Based on the nonlinear first-order shear deformation beam theory and the physical neutral surface concept, both the static and dynamic behaviors of FGM beams subjected to uniform in-plane thermal loading were derived by [Ma and Lee (2011)]. The thermo-elastic stresses in a three layered composite beam system with FGM layer were researched by [Nirmala, Upadhyay, Prucz and Lyons (2006)]. As for the research on the FMG plates, [Zhang and Zhou (2008)] presented a theoretical analysis to the FGM thin plates based on the physical neutral surface, in which the classical nonlinear laminated plate theory and the concept of physical neutral surface were employed to formulate the basic equations of the FGM thin plate. The elastic analysis for a thick cylinder made of FGMs was carried out by [Chen and Lin (2008)], and stress distributions along the radial direction were studied. The analytical solutions for the rotation problem of an inhomogeneous hollow cylinder with variable thickness under plane strain assumption was developed by [Zenkour (2010)], and for different types of the hollow cylinders, the analytical solutions of the elastic properties are given. Numerical investigations have also been carried out to study the thermo-elastoplastic behaviors of metal–ceramic FGMs by utilizing the method of finite element (FE) techniques [Giannakopoulos, Suresh, Finot and Olsson (1995); Finot and Suresh (1996); Weissenbek, Pettermann and Suresh (1997)].

It is worth mention that there is seldom work focus on the analytical solutions of the FGM plates subjected to the thermo-mechanical coupling. It has been reported by [Ekhlakov, Khay, Zhang, Sladek, Sladek and Gao (2012)] that the research on thermo-mechanical behaviors of FGMs subjected to thermo-mechanical coupling is important. Therefore, there is a strong need for an accurate analytical formulation to predict the thermo-mechanical behaviors of FGMs under different loadings such as thermal loading, pure bending and thermo-mechanical coupling. In order to get the theoretical solution, the averaging technique of composites are used to demonstrate the thermo-elastic behaviors of a three-layered FGM system under thermal loading, pure bending and thermo-mechanical coupling, respectively. When the temperature gradient and the bending moment vanish, the results can be degenerated to Liu's work [Liu, Dui and Yang (2013)]. Besides, this is one of the two parts work, this paper is focus on the thermo-elastic behaviors of the FGM system under thermal mechanical coupling, and the plastic work will be show in the next job.

2 Theoretical solutions for the FGMs under thermal loading

The coordinate axes and dimensions of the three-layered plate system can be illustrated in Fig. 1. The upper layer is the metallic phase, the lower layer is the ceramic layer and the middle layer of the system is the FGMs. Here we assumed that the interfaces of the FG-layers at $z = -a$ and $z = +a$ are continuous and be perfectly bonded at all times.

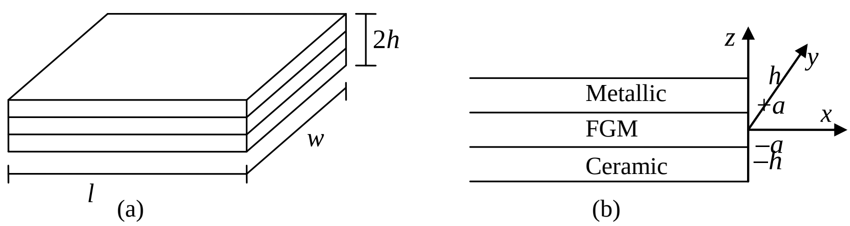

Figure 1: (a) Three-layered structural model and (b) coordinate axes and dimensions of the three-layered plate system.

In order to get the theoretical solution, a power function $V(z)$ which represents the volume fraction of the metallic phase is assumed to be the compositional gradation function of the FGM layer with a parameter 'm'. Hence, for a simple example, the following function of $V(z)$ can be considered as

$$V(z) = (\frac{z+a}{2a})^m. \tag{1}$$

And for different values of the parameter 'm', different graded distributions can be obtained. According to (1), for the boundary condition at the layers' interfaces, exist that,

$$V(z) = \begin{cases} 0 & z = -a \\ 1 & z = a \end{cases} \quad . \tag{2}$$

According to the small strain kinematics, the total strain of the thermo-elastic phase of the system can be composed of the elastic strain, ε_{ij}^{e}, and the thermal component, ε_{ij}^{the}, as

$$\varepsilon_{ij} = \varepsilon_{ij}^{e} + \varepsilon_{ij}^{the} \quad . \tag{3}$$

For the three layers system, under equal biaxial stress condition, exist that

$$\begin{array}{l} \sigma_{xx}(z) = \sigma_{yy}(z) = \sigma(z) \\ \varepsilon_{xx}(z) = \varepsilon_{yy}(z) = \varepsilon(z) \end{array} \quad . \tag{4}$$

Then the stress tensor and the strain tensor can be described as

$$\sigma_{ij} = \begin{pmatrix} \sigma(z) & 0 & 0 \\ 0 & \sigma(z) & 0 \\ 0 & 0 & 0 \end{pmatrix}, \quad \varepsilon_{ij} = \begin{pmatrix} \varepsilon(z) & 0 & 0 \\ 0 & \varepsilon(z) & 0 \\ 0 & 0 & \frac{-2\upsilon}{1-\upsilon}\varepsilon(z) \end{pmatrix}. \tag{5}$$

When the total strain of the system can be considered as a function of the out-of-plane coordinate, z, here we can define that ε_{0t} is the strain at the mid-plane of the FGM layer at $z = 0$, and it can be shown that the small strain compatibility equations lead to a linear relation between the total strain and curvature (K_{0t}), and the subscript '0t' represent the result of the system under thermal loading.

$$\varepsilon(z) = \varepsilon_{0t} + K_{0t} z. \tag{6}$$

Under plane stress conditions, the only non-zero stress component $\sigma(z)$ of the system can be given by

$$\sigma(z) = \frac{E(z)}{1-\upsilon}\left[\varepsilon_{0t} + K_{0t} z - a(z)\Delta T(z)\right], \tag{7}$$

where $E(z)$, $a(z)$ and υ represent the different Young's modulus, the coefficient of thermal expansion and the Poisson's ratio through the thickness of the three-layered system, respectively. Assumed that the number 1 represents the ceramic phase and the number 2 represents the metallic phase. Then for the ceramic phase, exist that $E(z) = E_1$, $a(z) = a_1$, $\upsilon = \upsilon_1$, and for the metallic phase, exist that $E(z) = E_2$, $a(z) = a_2$, $\upsilon = \upsilon_2$. In order to get the analytical solutions, here we assumed that $\upsilon_1 = \upsilon_2$. Assume that $\Delta T(z) = T_0 - T(z)$ represents temperature distributions through the thickness of the system, and if we assume a steady state distribution of temperature, $T(z)$ satisfies the difference principle, and assumed that the different temperatures in the multilayer system as

$$T\left(z\right)=\frac{T_1-T_0}{2h}z+\frac{T_1+T_0}{2}, \tag{8}$$

where $\Delta T\left(z\right)=T_0-T\left(z\right)$ and T_0 is the current temperature at the lower boundary of the system, T_1 is the current temperature of the upper boundary of the system. Then the stress distribution of the system can be obtained as the function ε_{0t}, K_{0t} and T_1 by averaging technique of composites, as

$$\sigma(z)=\begin{cases}\overline{E}_1\left[\varepsilon_{0t}+K_{0t}z-a_1\left(\frac{T_0-T_1}{2h}z+\frac{T_0-T_1}{2}\right)\right] \\ \text{for } -h\le z\le -a \\ \overline{E}_1\left[\varepsilon_{0t}+K_{0t}z-a_1\begin{pmatrix}\frac{T_0-T_1}{2h}z\\+\frac{T_0-T_1}{2}\end{pmatrix}\right]\left[1-V\left(z\right)\right]+V\left(z\right)\overline{E}_2\begin{bmatrix}\varepsilon_{0t}+K_{0t}z\\-a_2\begin{pmatrix}\frac{T_0-T_1}{2h}z\\+\frac{T_0-T_1}{2}\end{pmatrix}\end{bmatrix}, \\ \text{for } -a<z<a \\ \overline{E}_2\left[\varepsilon_{0t}+K_{0t}z-a_2\left(\frac{T_0-T_1}{2h}z+\frac{T_0-T_1}{2}\right)\right] \\ \text{for } a\le z\le h\end{cases} \tag{9}$$

where $\bar{E}_{i,i=1,2}=\frac{E(z)}{1-\upsilon}$. The expressions for ε_{0t} and K_{0t} can be derived by the boundary condition

$$\Sigma F_x=0 \text{ and also } \Sigma M_x=0. \tag{10}$$

Leads

$$\int_{-h}^{h}\sigma(z)dz=0,\quad \int_{-h}^{h}\sigma(z)zdz=0. \tag{11}$$

Substitute function (9) into (11), the following expressions can be obtained by

$$\begin{cases}\varepsilon_{0t}I_0+K_{0t}I_1-\left(J_0+R_1\right)=0\\ \varepsilon_{0t}I_1+K_{0t}I_2-\left(J_1+R_2\right)=0\end{cases}. \tag{12}$$

Results to

$$\begin{cases}\varepsilon_{0t}=\dfrac{\left(R_1+J_0\right)I_2-\left(J_1+R_2\right)I_1}{-I_1^2+I_0I_2}\\ K_{0t}=\dfrac{\left(J_0+R_1\right)I_1-\left(J_1+R_2\right)I_0}{I_1^2-I_0I_2}\end{cases}, \tag{13}$$

where

$$\begin{cases} (I_0, I_1, I_2) = \int\limits_{-h}^{h} \left(1, z, z^2\right) H(z)\, dz \\ (J_0, J_1) = \int\limits_{-h}^{h} (1, z) I(z)\, dz \\ (R_1, R_2) = \int\limits_{-h}^{h} \left(z, z^2\right) R(z)\, dz \end{cases}, \tag{14}$$

where

$$H(z) = \begin{cases} \bar{E}_1, & \text{for} \quad -h \le z \le -a \\ \bar{E}_1 \left[1 - V(z)\right] + \bar{E}_2 V(z) & \text{for} \quad -a \le z \le a \\ \bar{E}_2 & \text{for} \quad a \le z \le h \end{cases}, \tag{15}$$

$$I(z) = \begin{cases} \frac{\bar{E}_1 a_1 (T_0 - T_1)}{2} & \text{for} \quad -h \le z \le -a \\ \frac{\bar{E}_1 a_1 (T_0 - T_1)}{2} \left[1 - V(z)\right] + \frac{\bar{E}_2 a_2 (T_0 - T_1)}{2} V(z) & \text{for} \quad -a \le z \le a \\ \frac{\bar{E}_2 a_2 (T_0 - T_1)}{2} & \text{for} \quad a \le z \le h \end{cases}, \tag{16}$$

$$R(z) = \begin{cases} \frac{\bar{E}_1 a_1 (T_0 - T_1)}{2h} & \text{for} \quad -h \le z \le -a \\ \frac{\bar{E}_1 a_1 (T_0 - T_1)}{2h} \left[1 - V(z)\right] + \frac{\bar{E}_2 a_2 (T_0 - T_1)}{2h} V(z) & \text{for} \quad -a \le z \le a \\ \frac{\bar{E}_2 a_2 (T_0 - T_1)}{2h} & \text{for} \quad a \le z \le h \end{cases}. \tag{17}$$

And substituted (15-17) into (14), results can be got as

$$I_0 = \bar{E}_1 (h + a) + \bar{E}_2 (h - a) + (\bar{E}_2 - \bar{E}_1) \frac{2a}{m+1}$$

$$I_1 = \frac{\bar{E}_1 \left(a^2 - h^2\right)}{2} + \frac{\bar{E}_2 \left(h^2 - a^2\right)}{2} + (\bar{E}_2 - \bar{E}_1) a^2 \frac{2m}{(m+1)(m+2)}$$

$$I_2 = \frac{\bar{E}_1 \left(h^3 + a^3\right)}{3} + \frac{\bar{E}_2 \left(h^3 - a^3\right)}{3} + (\bar{E}_2 - \bar{E}_1) a^3 \frac{2\left(m^2 + m + 2\right)}{(m+1)(m+2)(m+3)}$$

$$J_0 = \frac{\bar{E}_1 a_1 (T_1 - T_0)}{2} (h + a) + \left[\begin{array}{c} \frac{\bar{E}_2 a_2 (T_0 - T_1)}{2} \\ -\frac{\bar{E}_1 a_1 (T_0 - T_1)}{2} \end{array} \right] \frac{2a}{m+1} + \frac{\bar{E}_2 a_2 (T_0 - T_1)}{2} (h - a)$$

$$\begin{aligned} J_1 = & \frac{\bar{E}_1 a_1 (T_0 - T_1)}{2} \frac{\left(a^2 - h^2\right)}{2} + \left[\begin{array}{c} \frac{\bar{E}_2 a_2 (T_0 - T_1)}{2} \\ -\frac{\bar{E}_1 a_1 (T_0 - T_1)}{2} \end{array} \right] \frac{2ma^2}{(m+1)(m+2)} \\ & + \frac{\bar{E}_2 a_2 (T_0 - T_1)}{2} \frac{\left(h^2 - a^2\right)}{2} \end{aligned}$$

$$R_1 = \frac{\bar{E}_1 a_1 (T_0 - T_1)}{2h} \frac{\left(a^2 - h^2\right)}{2} + \left[\begin{array}{c} \frac{\bar{E}_2 a_2 (T_0 - T_1)}{2h} \\ -\frac{\bar{E}_1 a_1 (T_0 - T_1)}{2h} \end{array} \right] \frac{2ma^2}{(m+1)(m+2)} + \frac{\bar{E}_2 a_2 (T_0 - T_1)}{2h} \frac{\left(h^2 - a^2\right)}{2}$$

$$R_2 = \frac{\bar{E}_1 a_1 (T_0 - T_1)}{2h} \frac{\left(h^3 + a^3\right)}{3} + \left[\begin{array}{c} \frac{\bar{E}_2 a_2 (T_0 - T_1)}{2h} \\ -\frac{\bar{E}_1 a_1 (T_0 - T_1)}{2h} \end{array} \right] \frac{2\left(m^2 + m + 2\right) a^3}{(m+1)(m+2)(m+3)} \frac{\bar{E}_2 a_2 (T_0 - T_1)}{2h} \frac{\left(h^3 - a^3\right)}{3} \tag{18}$$

For any application of the FGM system, the stress distribution of this model with different gradation parameter "m" can be obtained by using the general expressions of (9), (13) and (18) with the given material parameters. When the temperature distributions through the thickness of the system are assumed to be homogeneous, the work can be degenerate to Liu's work (2013).

3 Theoretical solutions for the FGMs under pure bending

This part is focus on the analytical solutions for the three layered system under pure bending. Assumed that the system is under isothermal environment with no thermal loading ($\Delta T(z) = 0$). According to (6), the stress component $\sigma(z)$ can be expressed by

$$\sigma(z) = \frac{E(z)}{1-\upsilon}[\varepsilon_{0b} + K_{0b} z], \tag{19}$$

where ε_{0b}, K_{0b} have the same physical significance as (6), while the subscript '0b' represent the corresponding values of the system under pure bending. Then in the similar way, the stress distribution of the system under pure bending can be expressed by

$$\sigma(z) = \begin{cases} \overline{E}_1(\varepsilon_{0b} + K_{0b} z) & -h \le z \le -a \\ \overline{E}_1(\varepsilon_{0b} + K_{0b} z)[1 - V(z)] + V(z)\overline{E}_2(\varepsilon_{0b} + K_{0b} z), & -a < z < a \\ \overline{E}_2(\varepsilon_{0b} + K_{0b} z) & a \le z \le h \end{cases}. \tag{20}$$

Due to the pure bending, the externally applied force is zero while the bending moment is not, then the expressions for ε_{0b} and K_{0b} can be derived by

$$\Sigma F_x = 0 \text{ and also } \Sigma M_x = M, \tag{21}$$

which lead to

$$\int_{-h}^{h} \sigma(z)dz = 0, \quad \int_{-h}^{h} \sigma(z)zdz = \frac{M}{L}. \tag{22}$$

Substituted Eq. (20) into Eq. (22),

$$\begin{cases} \varepsilon_{0b}I_0 + K_{0b}I_1 = 0 \\ \varepsilon_{0b}I_1 + K_{0b}I_2 = \frac{M}{L} \end{cases}, \tag{23}$$

where

$$(I_0, I_1, I_2) = \int_{-h}^{h} \left(1, z, z^2\right) H(z)\, dz, \tag{24}$$

and where $H(z)$ can be expressed as

$$H(z) = \begin{cases} \bar{E}_1 & \text{for} \quad -h \le z \le -a \\ \bar{E}_1\left[1 - V(z)\right] + \bar{E}_2 V(z) & \text{for} \quad -a \le z \le a \\ \bar{E}_2 & \text{for} \quad a \le z \le h \end{cases}. \tag{25}$$

And substituted (25) into (24), the solutions can be got as

$$\begin{aligned} I_0 &= \bar{E}_1 (h_0 + a) + \bar{E}_2 (h - a) + (\bar{E}_2 - \bar{E}_1) \frac{2a}{m+1} \\ I_1 &= \frac{\bar{E}_1 \left(h_0^2 - a^2\right)}{2} + \frac{\bar{E}_2 \left(h^2 - a^2\right)}{2} + (\bar{E}_2 - \bar{E}_1) a^2 \frac{2m}{(m+1)(m+2)} \\ I_2 &= \frac{\bar{E}_1 \left(h^3 + a^3\right)}{3} + \frac{\bar{E}_2 \left(h^3 - a^3\right)}{3} + (\bar{E}_2 - \bar{E}_1) a^3 \frac{2\left(m^2 + m + 2\right)}{(m+1)(m+2)(m+3)} \end{aligned}. \tag{26}$$

As a simple example for cases of different variations of $V(z)$ with different 'm', results of stress distributions of the system under pure bending can be obtained by (20, 23, 26) with the given material parameters.

4 Theoretical solutions for the FGMs under thermo-mechanical coupling

For the case of the system under thermo-mechanical coupling, with the different min-plane strain$\varepsilon_{0c}$and the laminate curvatureK_{0c}, the similar non-zero stress component $\sigma(z)$ can be given by

$$\sigma(z) = \frac{E(z)}{1 - \upsilon}\left[\varepsilon_{0c} + K_{0c}z - a(z)\Delta T\right]. \tag{27}$$

The subscript '$0c$' represents the corresponding values of the system under pure bending. The homogeneous temperature distribution in the multilayer system is the same as Eq. (8). Then the stress distribution of the system under varying temperature and the bending loads can be expressed as

$$\sigma(z)=\left\{\begin{array}{ll} \overline{E}_1\left[\varepsilon_{0c}+K_{0c}z-a_1\left(\frac{T_0-T_1}{2h}z+\frac{T_0-T_1}{2}\right)\right] & \text{for}\quad -h\le z\le -a \\ \overline{E}_1\left[\varepsilon_{0c}+K_{0c}z-a_1\left(\frac{T_0-T_1}{2h}z+\frac{T_0-T_1}{2}\right)\right]\left[1-V(z)\right] & \\ +V(z)\,\overline{E}_2\left[\varepsilon_{0c}+K_{0c}z-a_2\left(\frac{T_0-T_1}{2h}z+\frac{T_0-T_1}{2}\right)\right] & \text{for}\quad -a<z<a \\ \overline{E}_A\left[\varepsilon_{0c}+K_{0c}z-a_2\left(\frac{T_0-T_1}{2h}z+\frac{T_0-T_1}{2}\right)\right] & \text{for}\quad a\le z\le h \end{array}\right. . \tag{28}$$

Because the bending load is not zero, so the expressions for ε_{0c} and K_{0c} can be derived by

$$\Sigma F_x=0 \ \text{ and also } \ \Sigma M_x=\frac{M}{L}, \tag{29}$$

which lead to

$$\int_{-h}^{h}\sigma(z)dz=0,\qquad \int_{-h}^{h}\sigma(z)zdz=\frac{M}{L}. \tag{30}$$

Substitute Eq. (28) into Eq. (30), these can be integrated to produce

$$\left\{\begin{array}{l} \varepsilon_{0c}=\dfrac{(R_1+J_0)\,I_2-\left(J_1+R_2+{}^{M}\!/_{L}\right)I_1}{-I_1^2+I_0I_2} \\ K_{0c}=\dfrac{(J_0+R_1)\,I_1-\left(J_1+R_2+{}^{M}\!/_{L}\right)I_0}{I_1^2-I_0I_2} \end{array}\right. , \tag{31}$$

where

$$\left\{\begin{array}{l} (I_0,I_1,I_2)=\int\limits_{-h}^{h}\left(1,z,z^2\right)H(z)\,dz \\ (J_0,J_1)=\int\limits_{-h}^{h}(1,z)I(z)\,dz \\ (R_1,R_2)=\int\limits_{-h}^{h}\left(z,z^2\right)R(z)\,dz \end{array}\right. , \tag{32}$$

and

$$H(z)=\left\{\begin{array}{ll} \bar{E}_1, & \text{for}\quad -h\le z\le -a \\ \bar{E}_1\left[1-V(z)\right]+\bar{E}_2V(z) & \text{for}\quad -a\le z\le a \\ \bar{E}_2 & \text{for}\quad a\le z\le h \end{array}\right. , \tag{33}$$

$$I(z) = \begin{cases} \frac{\bar{E}_1 a_1 (T_0 - T_1)}{2} & \text{for} \quad -h \le z \le -a \\ \frac{\bar{E}_1 a_1 (T_0 - T_1)}{2} [1 - V(z)] + \frac{\bar{E}_2 a_2 (T_0 - T_1)}{2} V(z) & \text{for} \quad -a \le z \le a \\ \frac{\bar{E}_2 a_2 (T_0 - T_1)}{2} & \text{for} \quad a \le z \le h \end{cases}, \tag{34}$$

$$R(z) = \begin{cases} \frac{\bar{E}_1 a_1 (T_0 - T_1)}{2h} & \text{for} \quad -h \le z \le -a \\ \frac{\bar{E}_1 a_1 (T_0 - T_1)}{2h} [1 - V(z)] + \frac{\bar{E}_2 a_2 (T_0 - T_1)}{2h} V(z) & \text{for} \quad -a \le z \le a \\ \frac{\bar{E}_2 a_2 (T_0 - T_1)}{2h} & \text{for} \quad a \le z \le h \end{cases}. \tag{35}$$

And substituted (33-35) into (26), the solutions can be got as

$$\begin{aligned}
I_0 &= \bar{E}_1 (h + a) + \bar{E}_2 (h - a) + (\bar{E}_2 - \bar{E}_1) \frac{2a}{m+1} \\
I_1 &= \frac{\bar{E}_1 \left(a^2 - h^2\right)}{2} + \frac{\bar{E}_2 \left(h^2 - a^2\right)}{2} + (\bar{E}_2 - \bar{E}_1) a^2 \frac{2m}{(m+1)(m+2)} \\
I_2 &= \frac{\bar{E}_1 \left(h^3 + a^3\right)}{3} + \frac{\bar{E}_2 \left(h^3 - a^3\right)}{3} + (\bar{E}_2 - \bar{E}_1) a^3 \frac{2\left(m^2 + m + 2\right)}{(m+1)(m+2)(m+3)} \\
J_0 &= \frac{\bar{E}_1 a_1 (T_1 - T_0)}{2} (h + a) + \left[\begin{array}{c} \frac{\bar{E}_2 a_A (T_0 - T_1)}{2} \\ -\frac{\bar{E}_1 a_1 (T_0 - T_1)}{2} \end{array} \right] \frac{2a}{m+1} + \frac{\bar{E}_2 a_2 (T_0 - T_1)}{2} (h - a) \\
J_1 &= \frac{\bar{E}_1 a_1 (T_0 - T_1)}{2} \frac{\left(a^2 - h^2\right)}{2} + \left[\begin{array}{c} \frac{\bar{E}_2 a_2 (T_0 - T_1)}{2} \\ -\frac{\bar{E}_1 a_1 (T_0 - T_1)}{2} \end{array} \right] \frac{2ma^2}{(m+1)(m+2)} \\
&\quad + \frac{\bar{E}_2 a_2 (T_0 - T_1)}{2} \frac{\left(h^2 - a^2\right)}{2} \\
R_1 &= \frac{\bar{E}_1 a_1 (T_0 - T_1)}{2h} \frac{\left(a^2 - h^2\right)}{2} + \left[\begin{array}{c} \frac{\bar{E}_2 a_2 (T_0 - T_1)}{2h} \\ -\frac{\bar{E}_1 a_1 (T_0 - T_1)}{2h} \end{array} \right] \frac{2ma^2}{(m+1)(m+2)} \\
&\quad + \frac{\bar{E}_2 a_2 (T_0 - T_1)}{2h} \frac{\left(h^2 - a^2\right)}{2} \\
R_2 &= \frac{\bar{E}_1 a_1 (T_0 - T_1)}{2h} \frac{\left(h^3 + a^3\right)}{3} + \left[\begin{array}{c} \frac{\bar{E}_2 a_2 (T_0 - T_1)}{2h} \\ -\frac{\bar{E}_1 a_1 (T_0 - T_1)}{2h} \end{array} \right] \frac{2\left(m^2 + m + 2\right) a^3}{(m+1)(m+2)(m+3)} \\
&\quad + \frac{\bar{E}_2 a_2 (T_0 - T_1)}{2h} \frac{\left(h^3 - a^3\right)}{3}.
\end{aligned} \tag{36}$$

Then for cases of different variations of $V(z)$ with different 'm', results of stress distributions for the system under thermo-mechanical coupling can be obtained by (28, 31, 36) with the given material parameters.

5 Numerical results

In order to get the thermo-mechanical behaviors of the system, as a simple example, the system can be treated as a FGM thin plate made up of Ni-FGM- AL_2O_3layers, the upper layer is the isotropic elastic Ni, the lower layer is the isotropic AL_2O_3. In order to get the theoretical solutions, the FGM layer is assumed to be in the FGM layer with linear and quadratic and square variation of $V(z)$by substituting m=1, 2 and 0.5 into (18, 26, 36), respectively. For different cases of the system under thermal loading, pure bending and thermo-mechanical coupling, numerical results can be obtained by (9), (13), (18), (20), (23), (28), and (28), (31), (36). Here we assumed that all layers are isotropic elastic material, free of damage and having the temperature independent properties in Table 1 [Giannakopoulos, Suresh, Finot and Olsson (1995); Weissenbek, Pettermann and Suresh (1997)].

Table 1: Properties for the metallic (Ni) and ceramic (AL_2O_3) phases [Giannakopoulos, Suresh, Finot and Olsson (1995); Weissenbek, Pettermann and Suresh (1997)].

Material	$E_1(E_2)$	$a_1(a_2)$	$h_1(h_2)$	a	υ
AL_2O_3	380Gpa	$7.4{*}10^{-6\circ}C^{-1}$	0.405	0.285	0.25
Ni	214Gpa	$15.4{*}10^{-6\circ}C^{-1}$	0.655	0.285	0.25

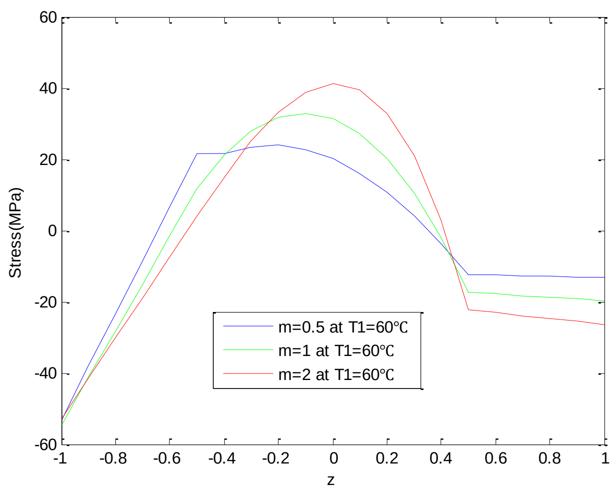

Figure 2: Analytical thermo-elastic stress distributions of the system with m=0.5, 1, 2 at T_0=200°C, T_1=60°C.

Fig. 2 shows the stress distributions through the thickness of the three-layered system under the pure thermal loading. The initial temperature is isotherm during the whole system with T_0= T_1=200°C, and the finial state is T_1=60 °C and T_0=200°C. The temperature gradient between the upper side and the lower side of the system can be determined by the different composition profiles with m=1, 2 and 0.5, respectively. As seen in Fig. 2, the case with m=2 shows a higher value of the stress in the Ni and FGM layer and a lower value of the stress in the AL_2O_3 layer than the other cases. So one can choose a smaller value of 'm' to lower the thermo-elastic stress of the FGM and metal layers, and choose a higher value of 'm' to lower the thermo-elastic stress of the AL_2O_3 layer. The results with m=1 from T_1=180°C to T_1=60°C can be shown in Fig. 3. As seen in Fig. 3, with the increasing thermal loadings, the stress distribution of the system shows a higher value.

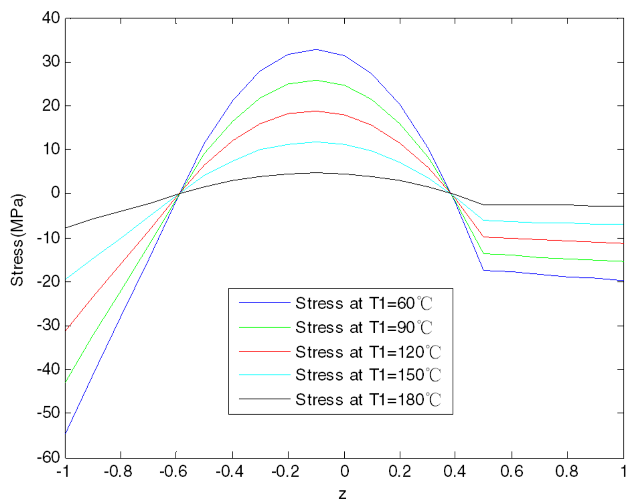

Figure 3: Analytical thermo-elastic stress distributions of the system with m=1 under different T_1.

Fig. 4 shows the stress distributions through the thickness of the three-layered system under different bending moment at uniform temperature circumstance with m=1. As seen in Fig. 4, the stress shows a higher value with the increasing bending moment. The stress distributions through the thickness of the three-layered system under pure bending with $M = 300$ for the different composition profiles at m=1, 2 and 0.5 can be shown in Fig. 5. It shows that there is little effect by the gradient function on the stress distribution of the FGM system under pure bending.

Fig. 6 shows the stress distributions through the thickness of the system under

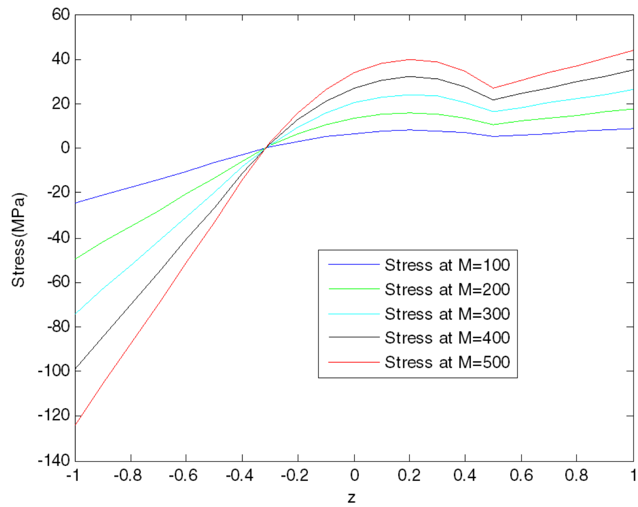

Figure 4: Analytical thermo-elastic stress distributions of the system with m=1 under different M.

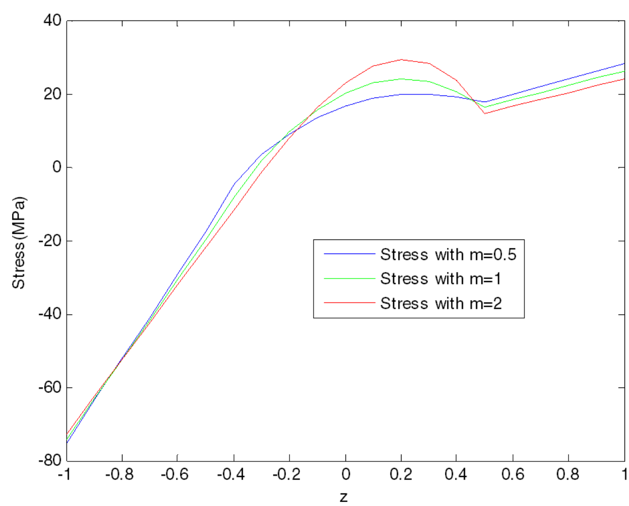

Figure 5: Analytical thermo-elastic stress distributions of the system with m=0.5, 1, 2 under M=300N·M.

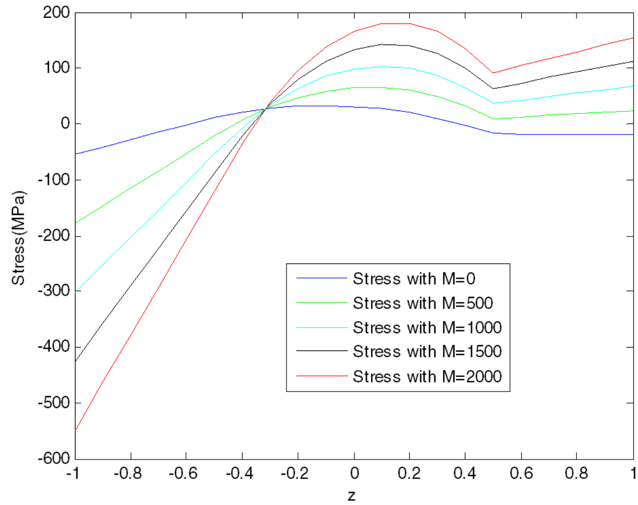

Figure 6: Analytical thermo-elastic stress distributions of the system under different bending moment with m=1 at T_0=200°C, T_1=60°C.

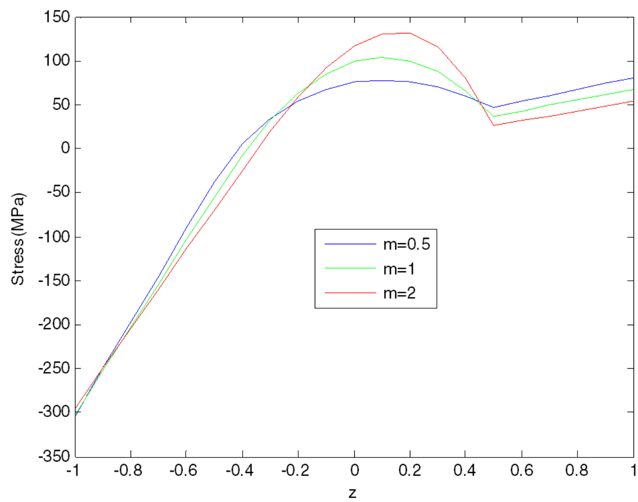

Figure 7: Analytical thermo-elastic stress distributions of the system with m=0.5, 1, 2 under M=1000N·M at T_0=200°C, T_1=60°C.

different bending moments at $T_0=200°C$and $T_1=60$ °C. As seen in Fig. 6, there is a higher stress with the increasing bending moment. The stress distributions through the thickness of the three-layered system with constant bending moment M=1000 and at $T_0=200°C$and $T_1=60$ °$C$for the different composition profiles with m=1, 2 and 0.5 can be shown in Fig. 7. Results of the system under the same bending moment$M$=1000 with m=1,$T_0=200°C$ and different T_1can be shown in Fig. 8. When the temperature gradient and the bending moment vanish, this model can be degenerated to Liu's model, and the stress distribution for the system with m=1 can be obtained in Fig. 9. The dot curve is Liu's work and the solid one is the present result. As shown in Fig.9, they agree very well with each other.

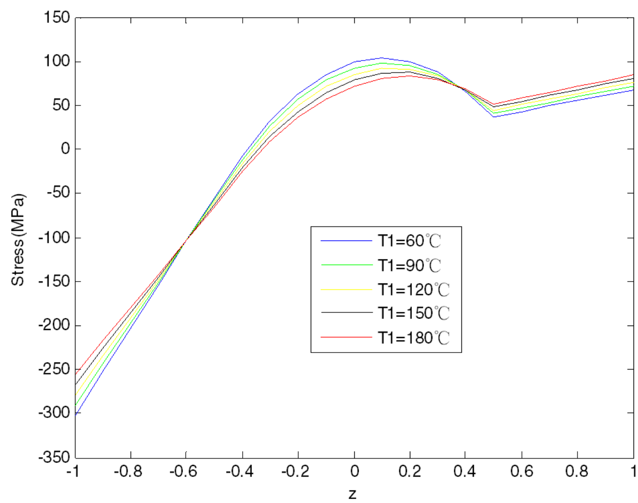

Figure 8: Analytical thermo-elastic stress distributions of the system with m=1, M=1000 N·M under different temperature distribution T_1.

6 Conclusions

The analytical solutions on the thermo-elastic stress solutions for FGMs under thermal loading, pure bending and thermo-mechanical coupling are studied in this work, respectively. The proposed relations for the stress distributions within a generic metal-FGM-ceramic system can predict accurately complex stress distributions induced by thermal loading, pure bending and thermo-mechanical coupling, respectively. By choosing the different appropriate FGM compositional gradation with linear, quadratic and square variations, the stress distribution within the sys-

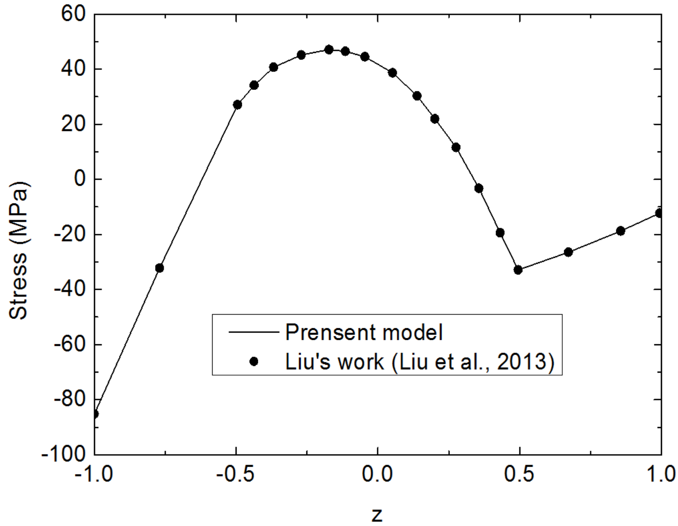

Figure 9: Analytical thermo-elastic stress distributions of the system with m=0.5, 1, 2 at ΔT=200°C.

tem can be controlled so that undesirable stresses at critical locations are minimized or avoided. The analytical thermo-elastic solutions presented here may be accounted for in many potential FGM composites design and can provide a simple, yet accurate tool for the prediction of thermally induced stresses in an FGM layer sandwiched between two homogeneous materials.

Acknowledgement: This work is supported by National Natural Science Foundation of China and Civil Aviation Administration of China jointly funded project (Grant # U1233106), the Fundamental Research Funds for the Central Universities funded project of Civil Aviation University of China (Grant # 3122014C015).

References:

Aboudi, J.; Pindera, M. J.; Arnold, S. M. (1994): Elastic response of metal matrix composites with tailored microstructures to thermal gradients. *Int. J. Solids. Struct.,* vol. 31, pp. 1393–428.

Birman. V.; Byrd, L. W. (2007): Modeling and Analysis of Functionally Graded Materials and Structures. *Appl. Mech. Rev.*, vol. 60, no. 5, pp. 195-216.

Bishay, P. L.; Atluri, S. N. (2013): 2D and 3D Multiphysics Voronoi Cells, Based on Radial Basis Functions, for Direct Mesoscale Numerical Simulation (DMNS) of the Switching Phenomena in Ferroelectric Polycrystalline Materials. *CMC: Computers Materials and Continua*, vol. 33, no. 1, pp. 19-62.

Chakraborty, A.; Gopalakrishnan, S.; Reddy, J. N. (2003): A new beam finite element for the analysis of functionally graded materials. *Int. J. Mech. Sci.*, vol. 45, pp. 519–39.

Chen, Y. Z.; Lin. X. Y. (2008): Elastic analysis for thick cylinders and spherical pressure vessels made of functionally graded materials. *Comput. Mater. Sci.,* vol. 44, pp. 581-588.

Dong, L.; El-Gizawy, A. S.; Juhany, K. A.; Atluri, S. N. (2014): A Simple Locking-Alleviated 4-Node Mixed-Collocation Finite Element with Over-Integration, for Homogeneous or Functionally-Graded or Thick-Section Laminated Composite Beams. *CMC: Computers Materials and Continua*, vol. 40, no. 1, pp. 49-76.

Dong, L.; El-Gizawy, A. S.; Juhany, K. A.; Atluri, S. N. (2014): A Simple Locking-Alleviated 3D 8-Node Mixed-Collocation C0 Finite Element with Over-Integration, for Functionally-Graded and Laminated Thick-Section Plates and Shells, with & without Z-Pins. *CMC: Computers Materials and Continua*, vol. 41, no. 3, pp. 163-192.

Ekhlakov, A.; Khay, O.; Zhang, C.; Sladek, J.; Sladek, V.; Gao, X. W. (2012): Thermoelastic crack analysis in functionally graded materials and structures by a BEM. *Fatigue & Fracture of Engineering Materials & Structures*, vol. 35, no. 8, pp. 742-766.

El-Hadek, M.; Tippur, H. V. (2003): Dynamic Fracture Parameters and Constraint Effects in Functionally Graded Syntactic Epoxy Foams. *International Journal of Solids Structures*, vol. 40, pp.1885–1906.

Finot, M.; Suresh, S. (1996): Small and large deformation of thick and thin 3lm multi-layers: effects of layer geometry, plasticity and compositional gradients. *J. Mech. Phys. Solids.,* vol. 44, no. 5, pp. 683–721.

Giannakopoulos, A. E.; Suresh, S.; Finot, M.; Olsson, M. (1995): Elastoplastic analysis of thermal cycling: layered materials with compositional gradients. *Acta Metall. Mater.,* vol. 43, no.4, pp. 1335–1354.

Huang, L. X.; Yao, Q.; Wang, L. (2011): An Inverse Analysis Algorithm of Material Parameters for Functional Graded Materials. *Advanced materials research*, vol. 243-249, pp. 6011-17.

Librescu, L.; Oh, S. Y.; Song, O. (2005): Thin-walled beams made of functionally graded materials and operating in a high temperature environment: vibration and stability. *J Therm. Stresses*, vol. 28, pp. 649-712.

Liu, B. F.; Dui, G. S.; Yang, S. Y. (2013): On the transformation behavior of functionally graded SMA composites subjected to thermal loading. *Eur. J. Mech. A-Solid.*, vol. 40, pp. 39-147.

Ma, L. S.; Lee, D. W. (2011): A further discussion of nonlinear mechanical behavior for FGM beams under in-plane thermal loading. *Comp. Struct.,* vol. 92, no. 2, pp. 831-842.

Miyamoto, Y.; Kaysser, W. A.; Rabin, B. H.; Kawasaki, A.; Ford, R. G. (1999): Functionally Graded Materials: Design, Processing and Applications. *KluwerAcademic Publishers*, Dordrecht.

Nirmala, K.; Upadhyay, P. C.; Prucz, J.; Lyons, D. (2006): Thermo-elastic Stresses in Composite Beams with Functionally Graded Layer. *J. Reinforced plastics and composites,* vol. 25, no. 12, pp. 1241-1254.

Sarkar, P.; Datta, S.; Nicholson, P. S. (1997): Functionally Graded Ceramic/Ceramic and Metal/Ceramic Composites by Electrophoretic Deposition, *Composites Part B*, vol. 28B, pp. 49–56.

Sun, K. H.; Hong, K.; Yuan, L. (2014): Inversion of Functional Graded Materials Elastic Properties from Ultrasonic Lamb Wave Phase Velocity Data Using Genetic Algorithm. *J. Nondestruct Eva,* vol. 33, no. 1 pp. 34-42.

Weissenbek, E.; Pettermann, H. E.; Suresh, S. (1997): Elasto-plastic deformation of compositionally graded metal–ceramic composites. *Acta Mater.,* vol. 45, no. 8, pp. 3401–3417.

Wu, C. C.; He, P. X.; Li, Z. (2002): Extension of J integral to dynamic fracture of functional graded material and numerical analysis. *Comp.&Strut.,* vol. 80, no. 5-6, pp. 411–416.

Yang, Q. Q.; Gao, C. F.; Chen, W. T. (2010): Stress analysis of a functional graded material plate with a circular hole. *Arch. Appl. Mech.,* vol. 80, no. 8, pp. 895–907.

Yang, J.; Chen, Y.; Xiang, Y.; Jia, X. L. (2008): Free and forced vibration of cracked inhomogeneous beams under an axial force and a moving load. *J. Sound. Vib.*, vol. 312, no. 1-2, pp. 166-181.

Zenkour, A. M. (2010): Rotating variable thickness inhomogeneous cylinders: part I-analytical elastic solutions. *Applied Mathematics*, vol. 1, pp. 481-488.

Zhang, D. G.; Zhou, Y. H. (2008): A theoretical analysis of FGM thin plates based on physical neutral surface. *Comput. Mater. Sci.,* vol. 44, pp. 716-720.

Zimmerman, R. W.; Lutz, M. P. (1999): Thermal stress and effective thermal expansion in a uniformly heated functionally graded cylinder. *J. Therm. Stress*, vol. 22, pp. 177–88.